RC22257 (W0111-065) November 21, 2001
Materials Science

IBM Research Report

Strain Relaxation Mechanisms in He^+- Implanted and Annealed $Si_{1-x}Ge_x$ Layers on Si(001) Substrates

Silke H. Christiansen, Patricia M. Mooney, Jack O. Chu, Alfred Grill
IBM Research Division
Thomas J. Watson Research Center
P.O. Box 218
Yorktown Heights, NY 10598

Research Division
Almaden - Austin - Beijing - Haifa - India - T. J. Watson - Tokyo - Zurich

LIMITED DISTRIBUTION NOTICE: This report has been submitted for publication outside of IBM and will probably be copyrighted if accepted for publication. Ithas been issued as a Research Report for early dissemination of its contents. In view of the transfer of copyright to the outside publisher, its distributionoutside of IBM prior to publication should be limited to peer communications and specific requests. After outside publication, requests should be filled only by reprints or legally obtained copies of the article (e.g. payment of royalties). Copies may be requested from IBM T. J. Watson Research Center , P. O. Box 218, Yorktown Heights, NY 10598 USA (email: reports@us.ibm.com). Some reports are available on the internet at http://domino.watson.ibm.com/library/CyberDig.nsf/home

Strain relaxation mechanisms in He^+-implanted and annealed $Si_{1-x}Ge_x$ layers on Si(001) substrates

S.H. Christiansen, P.M. Mooney, J.O. Chu and A. Grill
IBM T.J. Watson Research Center, Yorktown Heights, New York, USA

Abstract

Strain relaxation in He^+-implanted and annealed Si(001)/$Si_{1-x}Ge_x$ heterostructures was investigated using transmission electron microscopy techniques and x-ray diffraction. Depending on the implant conditions, bubbles and/or platelets form below the Si/$Si_{1-x}Ge_x$ interface upon annealing and act as nucleation sources for dislocation loops. The dislocation loops extend to the interface and form a misfit dislocation network there, resulting in relaxation of 30-80% of the strain in layers as thin as 100-300 nm. When bubbles form close to the interface, dislocations nucleate by a climb loop mechanism. When smaller bubbles form deeper in the Si substrate an irregular three-dimensional dislocation network forms below the interface resulting in an irregular misfit dislocation network at the interface. When platelets form deeper in the Si substrate, prismatic punching of dislocation loops is observed and dislocation reactions of misfit dislocations at the interface result in Lomer dislocation formation.

Introduction

Strain-relaxed $Si_{1-x}Ge_x$ layers on Si(001) substrates are used as virtual substrates for the epitaxial growth of active device layers of strained Si or $Si_{1-y}Ge_y$ ($y\neq x$) for SiGe-based high-speed transistors currently under investigation for high-speed digital and analog circuits [1-5]. Below the critical thickness for dislocation nucleation [6], a metastable, dislocation free, strained $Si_{1-x}Ge_x$ layer is maintained. Above the critical thickness, or upon annealing of a metastable layer, plastic relaxation occurs by the formation of a misfit dislocation network at the SiGe/Si interface. Since dislocations can only terminate at free surfaces, the misfit dislocations terminate in threading arms that run from the misfit segment through the $Si_{1-x}Ge_x$ layers to the wafer surface. The major challenge in using these virtual substrates is the control and reduction of threading dislocations that are unavoidably associated with misfit dislocations. The state of the art method to produce high quality relaxed
$Si_{1-x}Ge_x$ buffer layers with $x<0.35$ is the graded-buffer technique, i.e., the growth of step-graded or linearly graded $Si_{1-x}Ge_x$ layers that are several micrometers thick [3,7,8]. These graded $Si_{1-x}Ge_x$ buffer layers have threading dislocation densities on the order of 10^5-10^8 cm^{-2} and a typical peak-to-valley surface roughness of 20-50 nm, depending on the $Si_{1-x}Ge_x$ alloy composition and the grading rate [3,7,8]. Moreover, the relatively large $Si_{1-x}Ge_x$ layer thickness results in poor heat conduction, and a time-consuming, costly deposition [4,7].

An alternative approach to relaxed $Si_{1-x}Ge_x$ buffer layers has recently been proposed [9,10]. This involves a 3-step-process: the deposition of a thin metastable, dislocation free $Si_{1-x}Ge_x$ layer on a Si(001) substrate; the implantation of keV He ions below the $Si_{1-x}Ge_x$ /Si interface; and, finally, annealing at temperatures higher than 700 ^oC. A significant degree (30-80%) of strain relaxation in 100 nm-thick $Si_{1-x}Ge_x$ layers was achieved with a threading dislocation density comparable to that in graded buffer layers. Here we presented the results of a transmission electron microscopy (TEM) study of the strain relaxation mechanisms occurring for different implant conditions in implanted-annealed $Si_{1-x}Ge_x$ /Si structures.

Experimental Methods

Pseudomorphic $Si_{0.85}Ge_{0.15}$ and $Si_{0.80}Ge_{0.20}$ layers, were deposited by ultra-high vacuum chemical vapor deposition (UHVCVD). The layer thickness and alloy composition was measured by x-ray diffraction, which also showed that no strain relaxation had occurred during layer growth. The energy of the He^+ was chosen so that the projected range of the He atoms is below the Si/$Si_{1-x}Ge_x$ interface. Values for the implant depth were obtained from SRIM simulations [11]. To avoid channeling of the He^+-ions an incidence angle of 7^0 was used. The implant doses used were below the doses employed for Smart-Cut [12]. Annealing was done in a He ambient. The maximum degree of relaxation, measured by x-ray diffraction, was obtained after annealing at temperatures > 700 ^oC. The relaxation behavior of different implanted and annealed samples was evaluated using planar view (PVTEM) and cross sectional (XTEM) transmission electron microscopy.

Results and Interpretation

XTEM images taken after ion implantation show a band of implant damage in the Si substrate below the $Si/Si_{1-x}Ge_x$ interface. The width of this band, the straggle, is 50-80 nm, essentially independent of the implant depth and the dose. Upon annealing, the damage band vanishes and a well-defined layer of extended defects, platelets and/or bubbles of different sizes, is observed. Its position coincides with the center of the implant damage band in all samples.

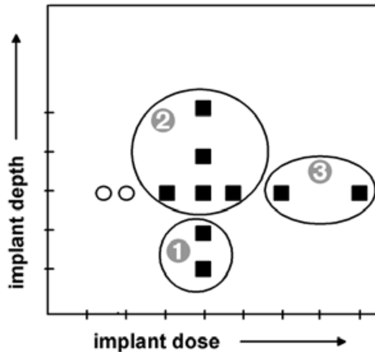

Fig.1: Degree of relaxation vs. implant does and depth: squares indicate relaxation 30-80%, empty circles indicate <10% relaxation. The relaxation mechanisms vary for the 30-80% relaxed samples.

Fig.1 shows a schematic of the degree of relaxation depending on the implant depth and dose. These parameters were varied systematically as indicated by the symbols on the plot. Circles indicate $Si_{1-x}Ge_x$ layers that relaxed only slightly (<10%) and were therefore not investigated any further. Squares indicate $Si_{1-x}Ge_x$ layers that relaxed by at least 30%. Evidence that the He implant is responsible for the high degree of strain relaxation is that the strain relaxation in regions of the same wafer that had not been implanted was negligible (<5%).

Although the degree of relaxation of the relaxed $Si_{1-x}Ge_x$ layer is almost independent of the implant depth and the dose, TEM analysis shows that strain relaxation occurs by different mechanisms for different implant conditions. The extended defects that form below the $Si/Si_{1-x}Ge_x$ interface upon annealing are bubbles in some samples (group 1 and group 3 in Fig. 1) and platelets in others (group 2 in Fig. 1). Both bubbles and platelets trigger dislocation nucleation. The dislocations glide towards the $Si/Si_{1-x}Ge_x$ interface where they form a misfit dislocation segment and thus relieve the strain in the $Si_{1-x}Ge_x$ layer. Under which conditions the bubbles and platelets form and how relaxation evolves will be discussed using TEM images of a selected sample from each group to illustrate the different relaxation mechanisms.

Bubble formation for shallow implants

Planar view and cross sectional TEM images of the samples with shallow implants show that bubbles form upon annealing. These bubbles reside at the $Si/Si_{1-x}Ge_x$ interface or slightly below it. A few bubbles are even found in the $Si_{1-x}Ge_x$ layer itself lying close to the interface. The diameter of these bubbles is ~30-40 nm. Fig. 2 shows a planar view micrograph under weak beam conditions of a sample of group 1 showing bubbles and misfit dislocations lying almost within one plane. For the shallower implant samples the bubbles at or slightly beneath the interface give rise to the nucleation of misfit dislocations outside of the bubbles. From this we infer that the bubbles must act as a kind of inclusion that causes strain in its vicinity. There is probably a high concentration (markedly different from equilibrium) of point defects around these bubbles. This is the case when the so-called trap mutation mechanism takes place [13-15].

The trap mutation mechanism requires the formation of a helium-vacancy defect (He-V) and subsequently the agglomeration of multiples of these complexes into He_n-V_m precipitates. When these precipitates have reached a critical size they transform into complexes that offer more space for the He by

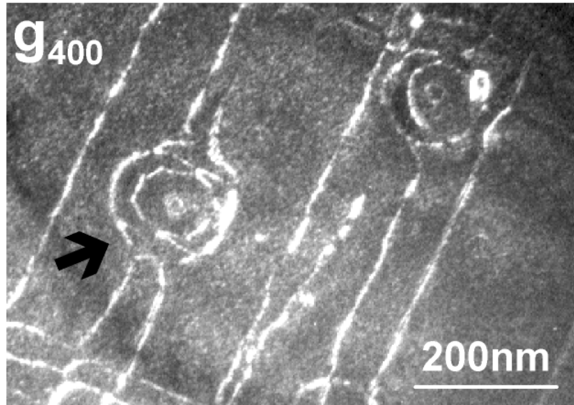

Fig. 2: Planar view TEM micrograph (weak beam conditions) of sample 1 from group 1 showing bubbles close to or slightly below the $Si/Si_{1-x}Ge_x$ interface together with a regular array of 60^0-misfit dislocations parallel to the <110>-directions at the Si/ $Si_{1-x}Ge_x$ interface. Some bubbles have dislocation loops around them (example is indicated by arrow).

pushing away the Si atoms. The self-interstitial that has been pushed away remains bound to the complex. Self-interstitials are known to cluster two-dimensionally. Thus, pushed out self-interstitials would do so and thereby favor the formation of dislocation loops. These dislocation loops immediately outside the precipitate surface extend in a plane perpendicular to the surface of the inclusion with a Burgers vector perpendicular to the plane of the loop [16]. The loop grows by the emission or absorption of point defects to become kidney shaped, i.e. it is a climb loop [16]. Eventually the extremities of the dislocation loop meet on the side of the precipitate and annihilate one another resulting in two loops that form concentric rings around the inclusion. The inner loop accommodates part of the misfit between inclusion and matrix. The outer loop does not accommodate misfit and is repelled. A slight modification of this climb loop mechanism results in the generation of dislocation spirals, namely as soon as a part of the growing, by then kidney shaped, loop moves upwards out of plane, another part moves downwards out of plane and the extremities of the loops will not meet. They will bypass one another and encircle the inclusion once more. This process is not unlikely since the outer part of the loop is unstable with respect to glide [17].

Fig. 2 shows examples of such a climb loop mechanism. One of the climb loops is still close to the He-inclusion and assumes the kidney shape stage of loop growth (indicated by arrow). In the deeper implant samples this climb loop mechanism is not observed. This is comprehensible since at a larger distance from the interface there is no glide force in the plane of the dislocation loops that could drive this process. However, the strain in the $Si_{1-x}Ge_x$ layer can push dislocation loops towards the interface where they relieve misfit strain as discussed in the next paragraph.

Platelet formation for deeper implants

For the samples having deeper implants (group 2 in Fig. 1), both platelets and bubbles form well below the interface. In these samples no bubbles reside at the interface or within the $Si_{1-x}Ge_x$ layer itself. The platelets are on the order of 100-150 nm-wide and have an average spacing of ~200 nm. The habit plane of the platelets is parallel to the $Si/Si_{1-x}Ge_x$ interface as shown in the cross sectional micrograph in Fig. 3. However, they also extend along either the <100>- directions or <110>-directions as visible in the planar view micrographs in Figs. 4 and 5. Those platelets that extend along <100>- directions in our samples

Fig. 3: Cross-sectional TEM micrograph (weak beam conditions) showing platelets below the $Si/Si_{1-x}Ge_x$ interface in sample 2 of group 2. From these platelets, dislocation loops extend in all 8 <110> directions and glide to form misfit dislocation segments at the interface as indicated by arrows.

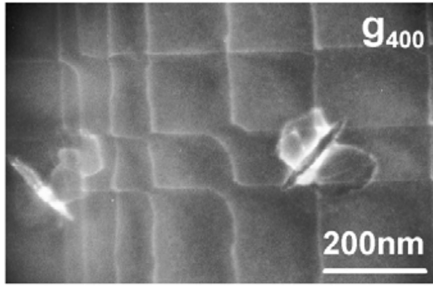

Fig. 4: Planar view TEM micrograph of sample 2 from group 2 (weak beam conditions) showing platelets along the <100> directions below the $Si/Si_{1-x}Ge_x$ interface along with a regular array of 60^0-misfit dislocations with line directions parallel to the <110>-directions at the interface.

usually give rise to so-called prismatic punching [16] of dislocation loops in the 8 possible <110>-directions as shown best in the cross section in Fig. 3. They are also visible in the planar view micrograph in Fig. 4. Platelets that extend along the <110>-directions are often related to an L-shaped crack or void. Between the two edges of the 'L'-shaped crack, dislocations extend. An example of such an 'L'-shaped crack is given in Fig 5. For all the platelets, the dislocations glide from the platelet towards the interface and form a misfit dislocation segment there. Figs. 3, 4 and 5 indicate that the platelets act as internal surfaces for the nucleation and termination of misfit dislocations.

Bubble formation for deeper implants at higher doses

For deeper implants at higher doses (group 3 in Fig. 1) again bubbles rather than platelets form as is visible in the planar view micrograph in Fig.6. The density of the bubbles is higher than the density of platelets; the bubbles have an average spacing of 30-40 nm. They are smaller in diameter than platelets, about 15-20 nm. Unlike the case of the group1 samples, the bubbles reside well below the $Si/Si_{1-x}Ge_x$ interface in the group 3 samples, as do the platelets in the group 2 samples. High-resolution micrographs of the bubbles (not shown) confirm their size and distribution as well as the shape that is faceted with {100}- and {110}-facet planes. Contrary to platelets, which each give rise to prismatic punching of dislocations, not all the bubbles below the interface induce enough strain to actually nucleate a dislocation. A lot of these bubbles below the $Si/Si_{1-x}Ge_x$ interface just trace dislocations. Since the bubbles are randomly distributed, the dislocation lines meander irregularly below the $Si/Si_{1-x}Ge_x$ interface and thus form a three-dimensional dislocation network. These dislocations are eventually driven towards the $Si/Si_{1-x}Ge_x$ interface where they form a regular misfit dislocation network consisting of 60^0dislocations that extend along the orthogonal <110>-directions. The misfit segments at the interface tend to be shorter for the higher dose samples (group 3) than for lower dose samples (group 2). However, the dislocation population at the interface is very similar for all samples, i.e. dominated by 60^0 misfit dislocations.

The misfit dislocation network

The overall misfit dislocation network at the interface is very similar for all the highly relaxed samples in the sense that the average misfit dislocation spacing is of the order of ~50-200 nm and consists of single dislocations rather than piled up dislocations as are found in graded buffer layers [3,8]. For the samples with

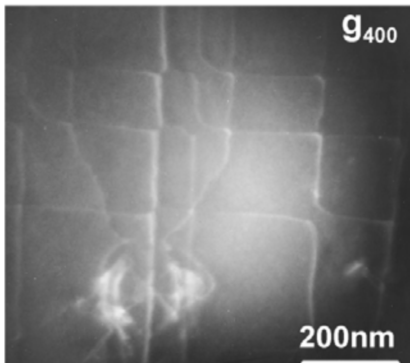

Fig. 5: Planar view TEM micrograph (weak beam conditions) of sample 2 from group 2 showing platelets along the <110> directions below the $Si/Si_{1-x}Ge_x$ interface together with a regular array of 60^0-misfit dislocations with line directions parallel to the <110>-directions at the interface.

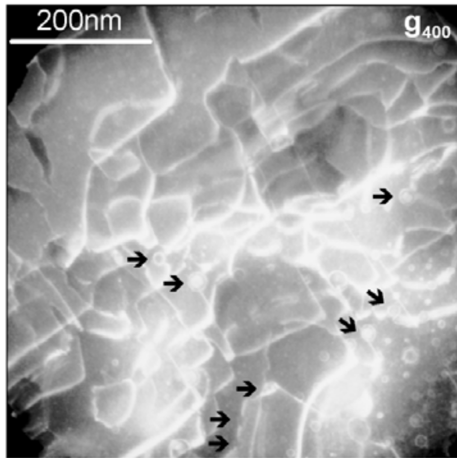

Fig. 6: Planar view TEM micrograph (weak beam conditions) of sample 3 from group 3. A large density of small bubbles form below the interface. Dislocations that meander between the bubbles lying below the interface are indicated by arrows. Dislocations eventually glide towards the interface where they form an array of 60^0 misfit dislocations parallel to the <110>-directions.

shallower implants (group 1), however, the regularity of the misfit dislocation network is less pronounced and can be locally disturbed by dislocations that pile up near bubbles that reside at the interface rather than below the interface. For the samples with deeper implants and lower implant doses (group 2) we observe, in addition to 60^0 misfit dislocations, pure edge dislocations, so-called Lomer dislocations [18,19], that are twice as effective in relieving strain as the usual mixed type 60^0-dislocations. These Lomer dislocations have an average spacing of ~1000 nm. Thus, they are ~10% of all misfit dislocations in this type of sample. No Lomer dislocations are observed in the low implant depth samples (group 1). This is probably due to the fact that the dislocation reaction of two 60^0-dislocations that is required for Lomer dislocation formation [19] is less likely to occur in samples having shallow implants.

Summary and Discussion

Dislocation formation in He implanted and annealed $Si/Si_{1-x}Ge_x$ structures is a complex phenomenon that occurs involving different processes or mechanisms such as He-clustering, bubble coalescence, trap mutation, dislocation loop punching, etc. These processes involve the interplay of radiation damage and diffusion of the He-implant atoms. The diffusion of He-implant atoms certainly depends on the strain fields that are active in the present samples. Strain originates from the lattice mismatch between the $Si_{1-x}Ge_x$ layer and the Si substrate and also from the He implant damage that tends to create high densities of self-interstitials and agglomerates in over-pressurized bubbles. Additional strain is contributed by the dislocations. The various strain components are different for different implant conditions and thus result in the different bubble/platelet and dislocation configurations observed. For the low dose and deep implant samples (group 2) we observe platelet formation in a confined layer, prismatic loop punching from platelets in 8 <110> directions and a regular misfit dislocation network at the interface containing 90% 60^0-dislocations as well as 10% Lomer dislocations. For the low dose and shallower implant samples (group 1) we see bubble formation in a confined layer at or slightly below the interface, dislocation glide loop nucleation and loop propagation within the $Si/Si_{1-x}Ge_x$ interface and a less regular misfit dislocation network at the interface containing 60^0-dislocations. Dislocation pileups at bubbles in the interface decrease the misfit dislocation network regularity. For the high dose samples (group 3) we see dense bubble formation in a confined layer below the interface, dislocation nucleation and propagation between bubbles resulting in an irregular three-dimensional dislocation network below the $Si/Si_{1-x}Ge_x$ interface and a regular misfit dislocation network at the interface containing 60^0-dislocations with misfit segments shorter than in the low dose samples (group 2).

Previous work on He ion implanted and annealed $Si/Si_{1-x}Ge_x$ structures has explored implant depths <100nm below the $Si/Si_{1-x}Ge_x$ interface and implant doses from $1x10^{15}cm^{-2}$ to $1x10^{17}cm^{-2}$ in order to achieve a high degree of strain relaxation [9,20]. We find that deeper implants and lower He doses result in a more regular misfit dislocation network at the interface, since dislocation pile ups at He-induced bubbles at the interface or even within the $Si_{1-x}Ge_x$ layer do not occur. It also allows for the prismatic punching mechanism to govern misfit dislocation formation and strain relaxation. This mechanism is different from the dislocation

mechanisms suggested to occur when the bubbles residing at or close to the interface give rise to dislocation nucleation [20]. The strain responsible for dislocation nucleation at extended platelets rather than at spherical bubbles is probably much higher.

Conclusion

We have shown that comparatively thin pseudomorphic $Si_{0.85}Ge_{0.15}$ and $Si_{0.80}Ge_{0.20}$ layers relax by implanting keV He^+-ions below the $Si/Si_{1-x}Ge_x$ interface and subsequent annealing. We have varied the implant conditions and have found that different relaxation mechanisms come into play. We find that platelet formation occurs for comparatively deep implants at a comparatively low dose. In constrast, bubbles form for higher doses or for shallower implants. The platelets initiate dislocation nucleation by prismatic loop punching, a mechanism which is not observed in the 'bubble regime'. The bubbles close to or at the interface nucleate dislocations by a climb loop mechanism. The bubbles deeper in the Si substrate nucleate dislocations at the highly defective material in the vicinity of the bubble. The misfit dislocation networks that form to relax the strain in the SiGe layer are in all cases regular, consisting essentially of 60^0 dislocations. In the platelet samples 60^0 misfit dislocations react and form ~10% Lomer dislocations.

Acknowledgement

The authors are grateful for the use of electron microscopes at the University of Erlangen-Nuremberg (Prof. H.P. Strunk) and at the IBM Microelectronics Division in East Fishkill, NY. S.H.C. is partially supported by a Feodor Lynen Fellowship awarded by the Alexander von Humboldt Foundation.

References

1. B.S. Meyerson, Proc. IEEE 80, 1592 (1992)
2. K. Ismail, S. Rishton, J.O. Chu and B.S. Meyerson, Electron Device Letters 14, 348 (1993)
3. P.M. Mooney, Materials Science and Engineering Reports R17, 105 (1996) and references therein
4. U. Konig, Mat. Res. Soc. Symp. Proc. 533, 3 (1998)
5. K. Rim, J.L. Hoyt and L.F. Gibbons, IEEE Trans. Electron Devices 47, 1406 (2000).
6. J.W. Matthew, A.E. Blakeslee, S. Mader, Thin Solid Films 33, 253 (1976)
7. E.A. Fitzgerald, Y.H. Xie, D. Monroe, P.J. Silverman, J.M. Kuo, A.R. Kortan, F.A. Thiel, B.E. Weir, J.Vac.Sci.Technol. B10, 1807 (1992)
8. F.K. LeGoues, B.S. Meyerson, J.F. Morara, Phys.Rev.Lett. 66, 2903 (1991)
9. D.M. Follstaedt, S.M. Myers, S.R. Lee, Appl.Phys.Lett. 69, 2059 (1996)
10. S. Mantl, B. Hollaender, R. Liedtke, S. Mesters, H.J. Herzog, H. Kibbel, T. Hackbarth, Nucl.Instr. and Meth. B147, 29 (1999)
11. J.F. Ziegler, J.P. Biersack, U. Littmark, The stopping and Range of Ions in Solids (Pergamon, New York, 1985)
12. M. Bruel, Nucl.Instr. and Meth. B108, 313 (1996)
13. A. VanVeen, J.H. Evans, L.M. Caspers, J.Th. DeHosson, J.Nucl.Mater. 12-123, 560 (1984)
14. L.M. Caspers, M. Ypma, A. VanVeen, G.J. Van des Kolk, phys.stat.sol. A63, K183 (1981)
15. E. Oliviero, M.F. Beaufort, J.F. Barbot, J.Appl.Phys. 90, 1718 (2001)
16. J.W. Matthews, in: Dislocations in solids 2, F.R.N. Nabarro, ed. North Holland Publishing Company, Amsterdam, New York, Oxford, 1979
17. G.R. Woolhouse, M. Ipohorski, Proc.Roy.Soc. A324, 415 (1971)
18. W.A. Lomer, Phil.Mag. 41, 1327 (1951)
19. V.I. Vdovin, L.A. Matveeva, G.N. Semenova, M.Ya. Skorohod, Yu.A. Tkhorik, L.S. Khazan, phys.stat.sol. (a) 92, 379 (1985)
20. M. Luysberg, D. Kirch, H. Trinkaus, B. Hollaender, S. Lenk, S. Mantl, H.J. Herzog, T. Hackbarth, P.F. Fichtner, Microscopy on Semiconducting Materials, IOP publishing, Oxford 2001, to be published